THE ASTROPHYSICAL JOURNAL, 389:L29–L32, 1992 April 10

THE STRUCTURE OF THE INNER ARCSECOND OF R AQUARII OBSERVED WITH THE *HUBBLE SPACE TELESCOPE*[1]

DENIS BURGARELLA AND FRANCESCO PARESCE[2]
Space Telescope Science Institute, 3700 San Martin Drive, Baltimore, MD 21218
Received 1991 October 25; accepted 1992 January 27

ABSTRACT

The inner arcsecond of R Aquarii has been observed with the faint object camera on the *Hubble Space Telescope* through the F120M filter centered on $\lambda = 1230$ Å. We use a simple and reliable linear deconvolution method to resolve the two features, designated C_1 and C_2 from radio observations, into several condensations. C_1 is composed of four objects, which we designate C_{1a}, C_{1b} located at 0.″099 from C_{1a}, C_3 at 0.″162 from C_{1a}, and C_4 at 0.″137 from C_{1a}. The source C_3, detected at 2 cm in the radio and in Hα using speckle interferometric techniques, might be the $V = 6$–11 Mira variable, observed at this wavelength because of the red leak. The nature of feature C_4, also detected in the radio but not with speckle techniques, is still unknown. Features C_{1a} and C_{1b} have not been resolved by any other instrument, and it might be possible that the hot star is one of the two or a nearby nondetected object. In the former case, we might be observing, for the first time, the rotation of the two stars forming the symbiotic system. C_2, lying to the northeast of these features, is also multiple and has a general shape that is consistent with a Herbig-Haro object.

Subject headings: binaries: symbiotic — circumstellar matter — ISM: jets and outflows — stars: individual (R Aqr) — ultraviolet: interstellar

1. INTRODUCTION

R Aquarii is a symbiotic system exhibiting a bright red continuum with strong TiO bands, a weak continuum in the blue, and high-excitation emission lines in the UV and optical. It is well accepted now (Allen 1988) that it is an interacting binary system. Infrared observations (Kenyon, Fernandez-Castro, & Stencel 1988) have shown that the cool star is a 387 day M7 Mira variable, with a radius of 300 $R_\odot$, a mass of ~ 1.5 $M_\odot$ (Burgarella, Vogel, & Paresce 1992), and a temperature of 2800 K (Anandarao & Pottasch 1986). From its effect on the surrounding matter, Burgarella et al. (1992) have deduced that the hot companion star should be a pre–white dwarf with $T_{\rm hot} \approx 40{,}000$ K and $\log g_{\rm hot} \approx 6.8$.

The inner nebula is constituted by a filamentary jet (Paresce et al. 1991) discovered by Wallerstein & Greenstein (1980). This feature has been studied at various wavelengths from X-rays (Viotti et al. 1987) to radio, but only recently VLA (Hollis, Dorband, & Yusef-Zadeh 1992), speckle interferometry (SI) by Hege, Allen, & Cocke (1991), and *Hubble Space Telescope* (*HST*) images (Burgarella et al. 1992) have resolved the structure of the two features C_1 and C_2.

In this *Letter*, we report on observations of the subarcsecond structure of R Aqr by using the high-resolution F120M images obtained with the faint object camera (FOC) on the *HST*. By doing so, we expect to obtain some information on C_1, which presumably contains the binary system, and C_2, which is the first detected feature associated with the jet.

2. OBSERVATION AND REDUCTION

R Aqr has been imaged with the FOC in the f/96 zoom mode on 1990 August 23 (Paresce et al. 1991). The field used in this work (Fig. 1) is part of the 22″ × 22″ image observed through the F120M filter, centered on $\lambda = 1230$ Å. The two features C_1 and C_2 are clearly separated and resolved into several subfeatures. C_2 is, apparently, a group of knots with a general northwest-southeast orientation, i.e., perpendicular to the jet. C_1 also appears to be multiple: a knot is resolved to the east of the bulk of C_1. The peak itself is not at the center of C_1 but is shifted to the north with two possible elongations to the southwest and southeast. Finally, a double-peaked knot is resolved to the southwest.

In the outer regions of the nebula, few photons were recorded during the 15 minute exposure time, and almost no information is available. In contrast to the situation described by Paresce et al. (1991), the FOC did not saturate with this filter, and the core of R Aqr appears clearly, as shown on the image in Figure 1. Simulations with FOCSIM (Paresce 1990) indicate that, owing to the strong red continuum of the M7 variable, a nonnegligible part of the flux from the Mira variable should be measured in the F120M filter because of the residual red leak. It is, however, difficult to estimate how much, because of the unknown reddening of the hot star. On the other hand, most ($\sim 80\%$) of the flux in the nebular structure is due to in-band UV flux.

The 1.″4 × 1.″4 central part of the raw F120M image is presented in the upper left-hand panel of Figure 2 (Plate L3). We first applied a 3 pixel × 3 pixel median filter to reduce the noise. In trying to enhance the resolution, we then applied a deconvolution technique to the medianized F120M image. The processing used the IRAF task Wiener (Hunt 1984). Noise is assumed to be white and is measured at the largest frequencies available in the image Fourier transform, where signal power is negligible with respect to noise power.

We selected the Wiener method for four reasons: (1) generally speaking, linear methods give sharper images than nonlinear ones (Adorf, Walsh, & Hook 1990); (2) we are not interested in the slow signal-to-noise pixels outside C_1, where

[1] Based on observations with the NASA/ESA *Hubble Space Telescope*, obtained at the STScI, which is operated by AURA, Inc., for NASA under contract NAS5-26555.

[2] Affiliated with the Astrophysics Division, Space Science Department of ESA.

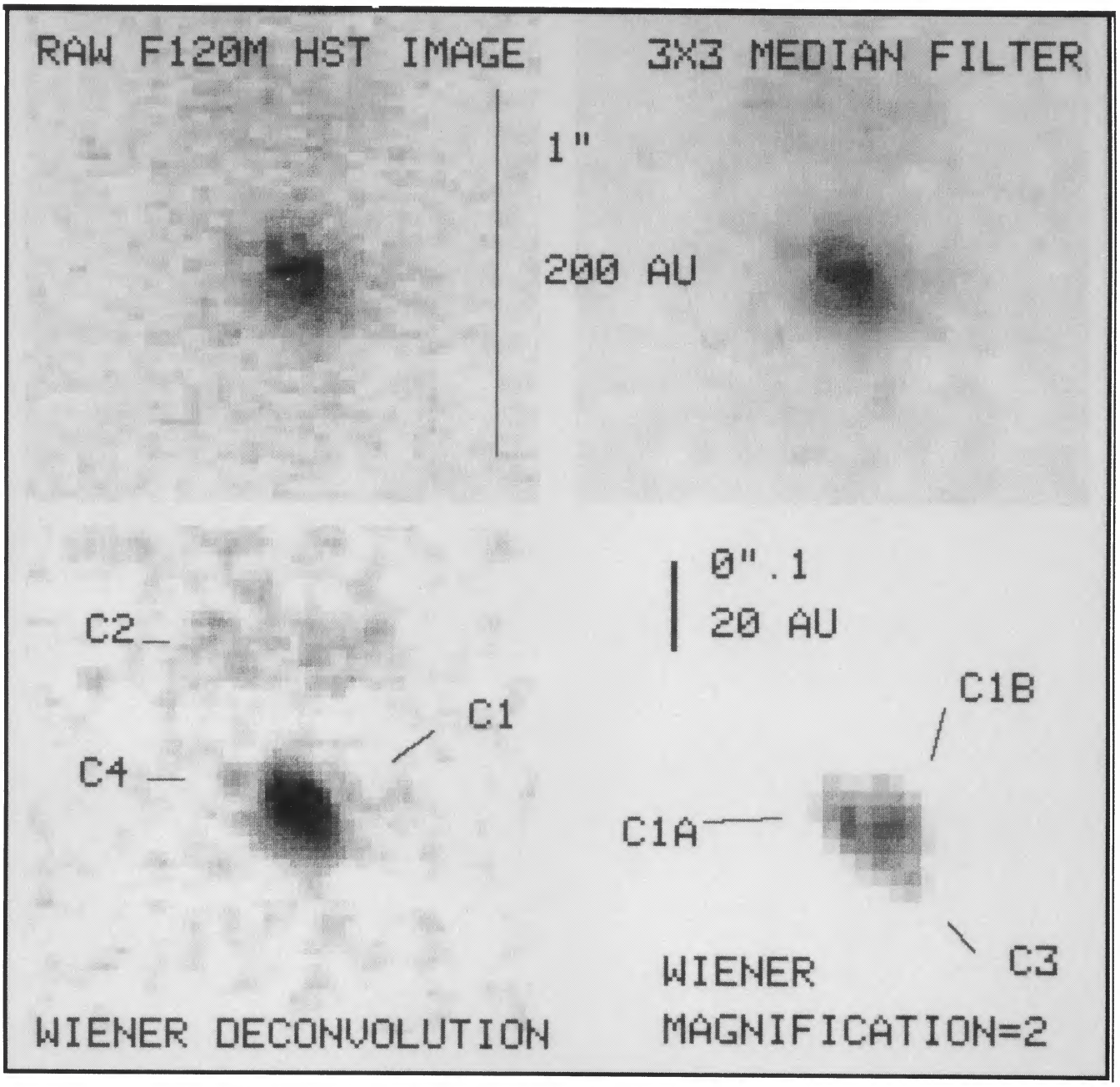

FIG. 2.—Inner 1".4 × 1".4 region of the F120M image. Each small square is a pixel of size 0".022. *Upper left:* raw F120M image; *upper right:* image after applying a 3 × 3 median filter; *lower left:* image after the Wiener deconvolution; *lower right:* deconvolved image magnified by a factor of 2 with a different cut to show the structure of C_1.

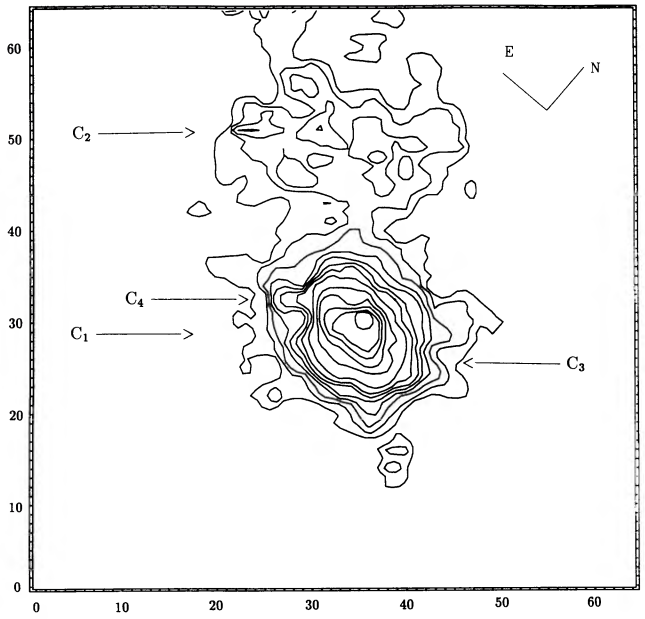

FIG. 1.—Contours showing the 64 pixel × 64 pixel (1".4 × 1".4) region of the F120M image. We clearly separate C_1 (*top*) and C_2 (*bottom*). Moreover, each of these features is resolved into several subfeatures that are discussed in the text. The contours are at 22.6%, 26.7%, 30.9%, 35.0%, 39.1%, 43.2%, 47.3%, 53.5%, 66.7%, 76.1%, 86.4%, 94.7%, and 99.2% of the peak count (24.3 counts).

the Wiener method may amplify the noise and is known to produce artifacts; (3) the Wiener method is a linear method and fluxes should be conserved; and (4) the algorithm is very simple and there is no need for many iterations. The processing time is just a few seconds. The point-spread function (PSF) used for this processing was obtained on 1990 September 9 (day 251) in the f/96 mode of the FOC. We present in Figure 3 the morphology of the PSF used for the deconvolution. The structure of the wings shows the usual concentric rings, while the core is very sharp as described by Greenfield et al. (1991).

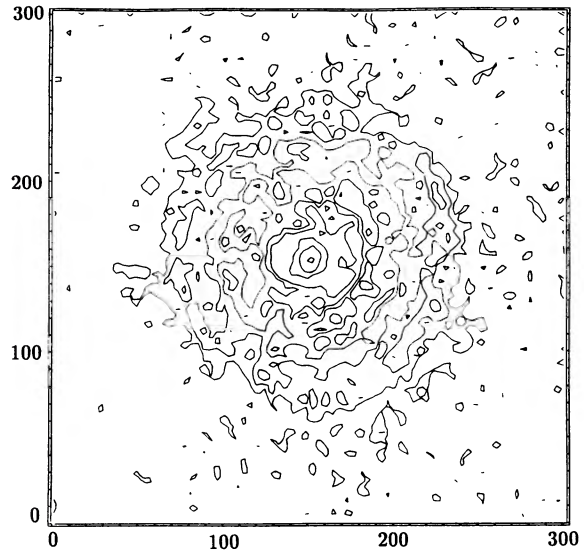

FIG. 3.—Contours showing the structure of the wings of the PSF. The scale is in pixels (~0".022). The contours are at 0.6%, 0.9%, 1.3%, 1.8%, 2.6%, 5.1%, 12.9%, and 51.4% of the peak count (389.05).

TABLE 1

LOCATIONS[a] AND FLUXES[b] OF THE DETECTED FEATURES IN C_1

Parameter	C_1[c]	C_{1a}[d]	C_{1b}[d]	C_3[d]	C_4[d]
ΔX (arcsec)	...	−0.033	0.033	0.129	−0.159
ΔY (arcsec)	...	−0.037	0.037	−0.021	−0.089
Flux[e] (counts)	5534.9	1631.0	1794.7	367.6	1212.0

[a] The geometric center of C_{1a} and C_{1b} has been arbitrarily taken as the origin, and we have put north at the top and east to the left after rotating the field by 50°.3 around the origin.

[b] After subtraction of the background.

[c] The flux of feature C_1 has been measured in the filtered F120M, before restoration, within a radius of 0".55.

[d] The flux of these features has been measured in the deconvolved image inside a radius of 3 pixels (0".066).

[e] The inverse sensitivity u is about 1.25×10^{-15}, and the exposure time is 900 s.

The result of the application of the Wiener method on the FOC field is very good, as shown in Figure 2. There is no noticeable amplification of the noise, while the resolution is clearly enhanced. We also notice that C_1 is clearly multiple (say, C_{1a}, C_{1b}, C_3, and C_4). For each detected feature, we present in Table 1 the shift in arcseconds in X (ΔX) and Y (ΔY) with respect to the geometric center of C_{1a} and C_{1b} in lines 1 and 2 and the number of counts in line 3. An interesting and easy check on the linearity of Wiener and how well this task did the job we wanted it to do can be performed with the data in Table 1. The sum of the counts corresponding to the four features detected is identical, within less than 10%, to the flux in C_1. This shows that Wiener is indeed quite linear. The flux from C_1 has been computed inside a radius of 0".55, while the fluxes of C_{1a}, C_{1b}, C_3, and C_4 have been measured within a radius of 3 pixels (0".066), which means that the light is now concentrated in a peak consistent with the resolution of *HST*.

The distance of R Aqr has been measured to be between 180 pc (Lépine, Le Squeren, & Scalise 1978; Solf & Ulrich 1985) and 250 pc (Whitelock 1987). We will, therefore, use $D = 200$ pc in this *Letter*. This means that 1" on R Aqr corresponds to 200 AU on our images.

3. DISCUSSION

The first important question about these results is: *Are these features real?* Hollis et al. (1992) have tried to deconvolve the saturated F501N image with a nonlinear maximum-entropy method. To address the problems produced by the very strong saturation, they apply a central mask to the dead pixels. The criterion used was that the slope in intensity from the external areas to the more central ones cannot decrease. This necessarily entails losing some information in the core of C_1.

Hollis et al. (1986) first resolved features C_1 and C_2 in the radio. In a new paper, Hollis et al. (1992) present what is the best available radio image of R Aqr. It represents the sum of four images over 4.5 yr with an equivalent exposure time of 25 hr. However, there may have been an evolution of C_1 and C_2 over this time. On the other hand, the global structure may not have changed. Assuming that C_1 is not resolved at 2 cm, this feature may be registered with the geometric center of C_{1a} and C_{1b}. In this case, feature C_4 is present in the radio, although not labeled as such, and there is an elongation of the radio feature C_1 in the direction of C_3. An Hα speckle interferometry image of R Aqr taken in 1983 is also presented by Hege et al. (1991). The claimed resolution is 45 mas, even better than the

PSF–aberrated FOC f/96 images. C_3 is shifted toward the south. In summary, it seems very likely that C_3 and C_4 are real and correspond to the previously detected features in radio (C_4) and SI (C_3), but C_{1a} and C_{1b} are newly resolved features and cannot be compared with previous observations.

Assuming that all the detected features are real and that C_1 is not resolved either in the radio or with the SI observation, we obtain the following results. For a 1.5 $M_\odot$ Mira variable, a 1.0 $M_\odot$ hot companion, and the possible 44 yr orbital period (Willson et al. 1981), Kepler's third law yields a separation of about 17 AU, or 4 pixels. The distances between the features in C_1 are comparable to this separation. If the binary system is inside C_1, we have, therefore, certainly resolved it, but the second important question is, *where is it?*

The nature of C_4 is completely unknown. This feature has already been detected by Hollis et al. (1992) with the VLA, but Hege et al. (1991) did not report C_4 with the SI method. There is an elongation in C_1 roughly to the east, which they refrained from overinterpreting and which cannot be mistaken for C_4 (Hege 1991). The locations of C_4 on the radio and *HST* images are very close, and, if this object has moved, the movement is too small to be detectable. The source called C_3 is resolved in speckle and with the *HST* deconvolved images. This feature is interpreted as being the long-period variable (LPV) by Hege et al. (1991). This is approximately consistent with the astrometric optical positions of the LPV measured by Baudry et al. (1990) and Michalitsianos et al. (1988) and with the SiO maser position (Wright et al. 1990). These three determinations have been put by Hollis et al. (1990) in the common epoch (1988.12), after correction for the proper motion, and are shown in Figure 4.

We have put in Figure 4 the radio and SI features C_1 at the same location, corresponding to the geometric center of C_{1a} and C_{1b}. The SiO maser's position estimated errors are about $\pm 0''.15$ in right ascension and $0''.20$ in declination. The position of the SiO maser, even if we account for these uncertainties, is, therefore, far away from C_3 at a distance of about $0''.2$. The estimated uncertainties of Baudry et al.'s (1990) optical position are about $\pm 0''.10$ in right ascension and $0''.20$ in declination. Michalitsianos et al.'s (1988) uncertainties are about $0''.04$ in right ascension and $0''.05$ in declination, which may be a little bit optimistic, due to uncertainties in the FK4 and the proper motions, and should be of the same order as Baudry et al.'s estimates. The LPV and SiO positions are shifted toward the southwest with respect to the position of C_3, but C_3 is within the error box determined by Baudry et al. (1990), while it is close to the error box determined by Michalitsianos et al. (1988). It seems, therefore, possible that C_3 is the Mira variable and that the variation of position between the 1983 SI and the 1990 *HST* locations is due to the rotation of the binary system observed for the first time. C_{1a} or C_{1b} may be the hot companion star or, at least, some gas orbiting around it. Effectively, if C_3 is the LPV, the hot star has to be somewhere around it, within $\sim 0''.1$ from Kepler's third law. These features are, therefore, the only possible candidates if we assume that some flux from the 40,000 K star (Burgarella et al. 1992) shines through the F120M filter. Other arguments are proposed by Hege et al. (1991). If we assume that the SiO source should be close to the stellar atmosphere of the LPV (see Baudry et al. 1990 for a discussion), however, we may take the average position of the LPV (Michalitsianos et al. 1988; Baudry et al. 1990) plus the SiO maser (Wright et al. 1990) as the best estimate of the location of the Mira. In this case, C_3 is off by about $0''.15$.

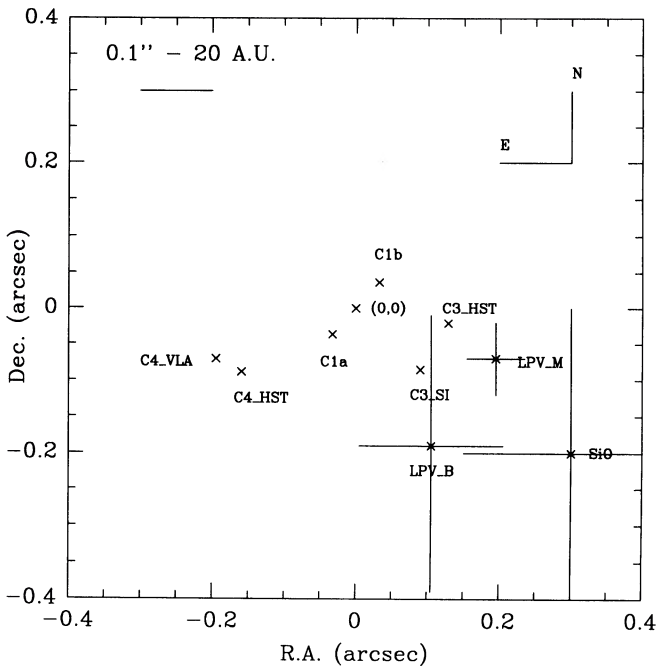

FIG. 4.—Locations of the different features detected in or close to feature C_1 with different instruments. The 2 cm radio VLA (Hollis et al. 1992) and Hα speckle interferometry (Hege et al. 1991) features C_1 (0, 0) have been superposed to the geometric center of C_{1a} and C_{1b}, taken for the origin. The positions of the *HST* features, after rotation to put north at the top and east to the left, are from Table 1 (epoch 1990.64). The radio VLA locations (Hollis et al. 1992) of the resolved features are from an average image from 1984 to 1987 (mean epoch 1985.64). The speckle position is from Hege et al. (1991) (epoch 1983.79). The LPV astrometric positions are indicated by LPV_B (epoch 1987.06) for Baudry et al.'s (1990) position and LPV_M (epoch 1986.68) for Michalitsianos et al.'s (1988) position. Finally, the SiO position (epoch 1988.12) is determined by Wright et al. (1990).

The structure of C_2 seems to be changing with time (Hollis et al. 1986; Hege et al. 1991). Burgarella et al. (1992) show that C_2 is knotty and filamentary at the same time, as are Herbig-Haro (HH) objects (see HH 34 in Reipurth et al. 1986, for instance), but in contrast to regular HH objects (Mundt 1987), the radio spectral index (using the convention $F \approx \nu^\alpha$) is apparently negative (Burgarella et al. 1992). Several models have been proposed to explain the HH objects (Dyson 1987), but a rather common feature is the collision of a very collimated hypersonic stellar wind on interstellar gas or the collision of a condensation with circumstellar gas. The former is consistent with the *HST* images and with the results from Solf (1991), which show that the shapes of the lines emitted in the northeast jet of R Aqr are similar to those of HH objects. The shock velocity in the outer feature A may be as high as 500 km s^{-1}. Thus, we find very likely, as suggested by Solf (1991), that a very collimated stellar wind produced in the core of R Aqr hits existing condensations along its way out and then forms HH objects. It is, however, quite difficult to establish the exact origin of the jet itself (Burgarella et al. 1992).

4. CONCLUSION

Using the F120M FOC/*HST* images, we have resolved the core of the symbiotic system R Aqr into four objects that we call C_{1a}, C_{1b}, C_3, and C_4. Two of them, C_3 and C_4, have been separately detected by speckle interferometry and 2 cm radio imagery, respectively. The deconvolved image of C_3 may be the

Mira variable or its extended atmosphere. On the other hand, the astrometric optical position of the Mira does not match very well the position of C_3 if the SiO maser is emitted close to the stellar atmosphere of the LPV. All of this assumes, as Hege et al. (1991) and Hollis et al. (1992) have done, that the C_1 optical emission coincides with the radio feature C_1.

The precise nature of C_{1a}, C_{1b}, and C_4 is for the moment unknown, but it might be possible, if the Mira is in C_3, that the hot star is either one of the C_{1a} and C_{1b} features or, at least, very close to them. The shape of C_2 is very similar to that of HH objects produced by the collision of a collimated wind with circumstellar matter. More high-resolution observations are urgently needed to confirm the existence of these features. It would be very interesting to use the spectroscopic capabilities of *HST* to observe the core of R Aqr. If two of the resolved objects really are the two stars, their spectra would identify them unambiguously.

We are very grateful to the referee, E. K. Hege, for his valuable comments and to R. J. Hanisch for his help in the deconvolution. D. B. thanks the ESA for a postdoctoral fellowship.

REFERENCES

Adorf, H.-M., Walsh, J. R., & Hook, R. N. 1990, in Proc. Workshop on the Restoration of *HST* Images and Spectra, ed. R. L. White & R. J. Allen (Baltimore: STScI), 121
Allen, D. 1988, in IAU Colloq. 103, The Symbiotic Phenomenon, ed. J. Mikolajewska, M. Friedjung, S. J. Kenyon, & R. Viotti (Dordrecht: Kluwer), 3
Anandarao, B. G., & Pottasch, S. R. 1986, A&A, 162, 167
Baudry, A., Mazurier, J. M., Perié, J. P., Requième, Y., & Rousseau, J. M. 1990, A&A, 232, 258
Burgarella, D., Vogel, M., & Paresce, F. 1992, A&A, in press
Dyson, J. E. 1987, in IAU Symp. 122, Circumstellar Matter, ed. I. Appenzeller & C. Jordan (Dordrecht: Reidel), 159
Greenfield, P., et al. 1991, in Proc. SPIE Conf. on Space Astronomical Telescopes and Instruments, 1494, 16
Hege, E. K. 1991, private communication
Hege, E. K., Allen, C. K., & Cocke, W. J. 1991, ApJ, 381, 543
Hollis, J. M., Dorband, J. E., & Yusef-Zadeh, F. 1992, ApJ, 386, 293
Hollis, J. M., Michalitsianos, A. G., Kafatos, M., Wright, M. C. H., & Welch, W. J. 1986, ApJ, 309, L53
Hollis, J. M., Wright, M. C. H., Welch, W. J., Jewell, P. R., Crull, H. E., Kafatos, M., & Michalitsianos, A. G. 1990, ApJ, 361, 663
Hunt, B. R. 1984, Digital Image Processing Techniques, ed. M. P. Ekstrom (New York: Academic), 53
Kenyon, S. J., Fernandez-Castro, T., & Stencel, R. E. 1988, AJ, 95, 1817
Lépine, J. R. D., Le Squeren, A. M., & Scalise, E. 1978, ApJ, 225, 869
Michalitsianos, A. G., Oliversen, R. J., Hollis, J. M., Kafatos, M., Crull, H. E., & Miller, R. J. 1988, AJ, 95, 1478
Mundt, R. 1987, in IAU Symp. 122, Circumstellar Matter, ed. I. Appenzeller & C. Jordan (Dordrecht: Reidel), 147
Paresce, F. 1990, Faint Object Handbook, Version 2.0, Space Telescope Science Institute.
Paresce, F., et al. 1991, ApJ, 369, L67
Reipurth, B., Bally, J., Graham, J. A., Lane, A. P., & Zealey, W. J. 1986, A&A, 164, 51
Solf, J. 1991, A&A, in press
Solf, J., & Ulrich, H. 1985, A&A, 148, 274
Viotti, R., Piro, L., Friedjung, M., & Cassatella, A. 1987, ApJ, 319, L7
Wallerstein, G., & Greenstein, J. L. 1980, PASP, 92, 273
Whitelock, P. A. 1987, PASP, 99, 573
Willson, L. A., Garnavich, P., & Mattei, J. 1981, Inf. Bull. Var. Stars, No. 1961
Wright, M. C. H., Carlstrom, J. E., Plambeck, R. L., & Welch, W. J. 1990, AJ, 99, 1299

PLATE L2

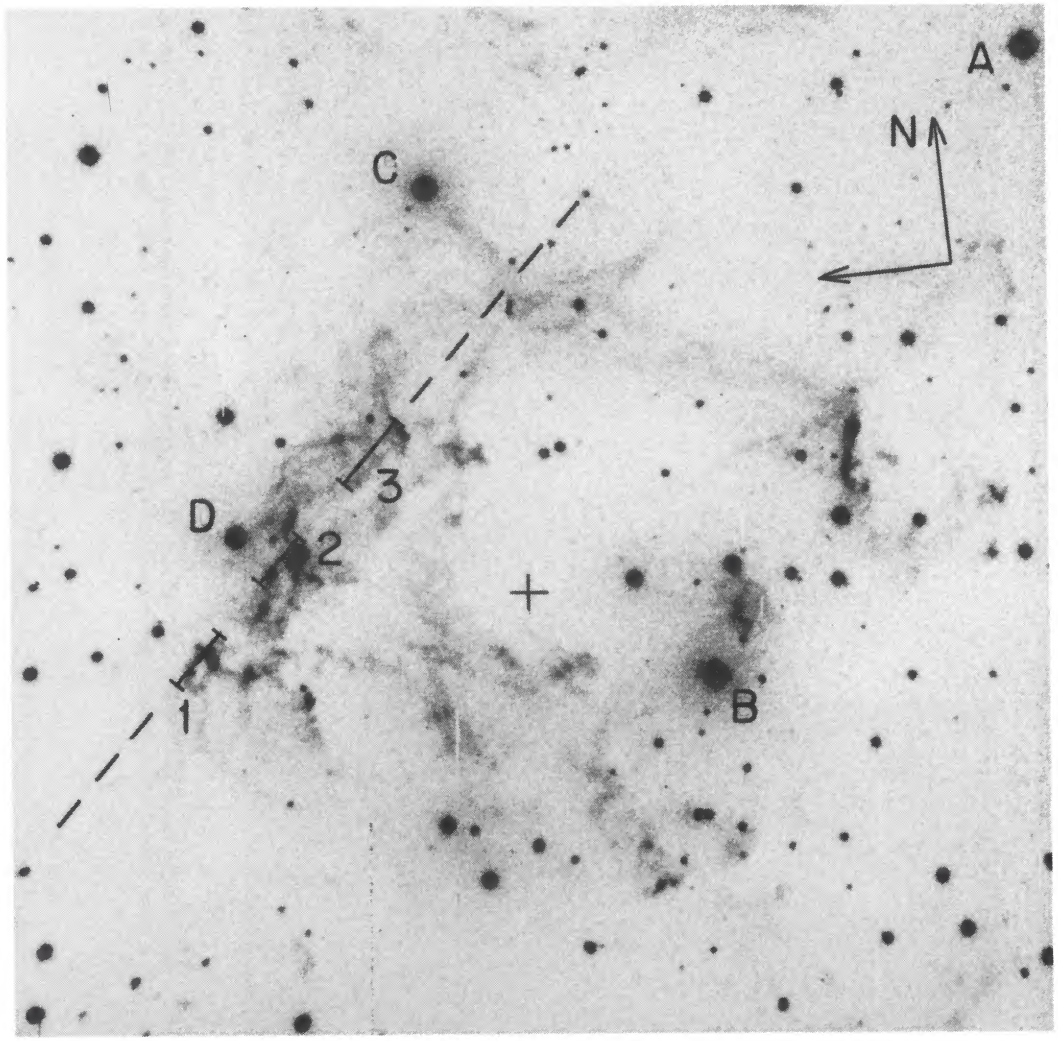

FIG. 2.—CCD image of the SNR G203.2−12.3 in the light of [S II] (same image as in Fig. 1*b*, but with reference stars and accurate directions of north and east indicated). See Table 2 for star coordinates. The plus sign indicates the nominal center of the SNR. The spectrograph slit location is also shown; one-dimensional spectra have been extracted at the positions denoted 1–3 along the slit.